Evolution of anisotropy of a partonic system from relativistic heavy-ion collisions

Weronika Jas*
Institute of Physics, Świętokrzyska Academy ul. Świętokrzyska 15, PL-25406 Kielce, Poland

Stanisław Mrówczyński†
Institute of Physics, Świętokrzyska Academy ul. Świętokrzyska 15, PL-25406 Kielce, Poland and
Sołtan Institute for Nuclear Studies ul. Hoża 69, PL-00681 Warsaw, Poland
(Received 4 July 2007; published 10 October 2007)

The evolution of anisotropy in momentum and coordinate space of the parton system produced in relativistic heavy-ion collisions is discussed within the free-streaming approximation. The momentum distribution evolves from the prolate shape (elongated along the beam) to the oblate one (squeezed along the beam). At the same time, the eccentricity in coordinate space, which occurs at finite values of impact parameter, decreases. It is argued that the parton system reaches local thermodynamic equilibrium before the momentum distribution becomes oblate.

DOI: 10.1103/PhysRevC.76.044905 PACS number(s): 25.75.−q, 12.38.Mh

I. INTRODUCTION

A parton system, which emerges at the early stage of relativistic heavy-ion collisions, is anisotropic both in momentum and coordinate space. These anisotropies crucially influence the dynamics of the system: the momentum one causes plasma color instabilities (for a review, see Ref. [1]); the coordinate space one is responsible for hydrodynamic elliptic flow (for a review, see Ref. [2]). An eccentricity of the overlap region of colliding nuclei at nonzero impact parameter decreases when the parton system produced in the overlap region expands. While the eccentricity simply decays, the parton momentum distribution, which is observed locally, changes from a strongly prolate shape (elongated along the beam axis) to an oblate form (squeezed along the beam).

Since hydrodynamics requires at least partial local equilibrium [3], an observation of the elliptic flow suggests that the parton system is thermalized before the initial eccentricity is significantly reduced. The equilibration time of the parton system $t_{\rm eq}$ was actually estimated to be shorter than 1 fm/c [4]. Interparton collisions cannot equilibrate the system so fast, but magnetic unstable modes due to the momentum anisotropy speed up the equilibration process. However, the question arises as to whether the momentum distribution is prolate or oblate just before equilibrium is reached. In this paper, we attempt to resolve the issue in a very simple classical model where partons produced in the overlapping region of colliding nuclei freely escape from it. We analyze how the coordinate space anisotropy decays and how the momentum distribution evolves in a box which includes the Lorentz contracted region where the partons are initially produced. The effect of finite formation time of produced partons is taken into account.

We are fully aware of how naive our approach is. Matter, which emerges at the early stage of relativistic heavy-ion collisions, is very dense, presumably inhomogeneous, and partially coherent because of the memory of the pure quantum state of two colliding nuclei. Such a system cannot be reliably described in terms of kinetic theory with weakly interacting quasiparticles on mass-shell. A derivation of the transport equation from quantum field theory clearly reveals the limitations of the kinetic approach [5]. We believe, however, that our free-streaming model still grasps the global features of the early stage system. The evolution of anisotropies, which is our main interest here, is dominated by the system's expansion. And it proceeds with the velocity of light independently of details of the system's dynamics. However, it should be clearly understood that in the free-streaming model, where no interaction is present, a real equilibration does not take place. Therefore, even if the particle momentum distribution appears to be of the equilibrium form, one cannot conclude that the system has reached equilibrium, which is required by the hydrodynamic description, as the pressure resulting from interparticle collisions is absent in the free-streaming model. We will return to this discussion in the concluding section of the paper.

II. DECAY OF ECCENTRICITY

The partons are assumed to be produced in an ellipsoidal region parametrized by the three-dimensional Gaussian function centered at zero with the widths σ_x, σ_y, and σ_z, where x, y, and z denote Cartesian coordinates. As usual, the z axis is along the beam. The distribution of parton rapidity, which is denoted here by Y, is also assumed to be Gaussian with the width ΔY. We note that the rapidity distribution of charged pions produced in Au-Au collisions at $\sqrt{s} = 200$ GeV per nucleon-nucleon pair is well described by the Gaussian distribution with $\Delta Y = 2.3$ [6]. Since we work in the center-of-mass frame, the rapidity distribution is centered at zero. We also assume that partons are massless, and then, as will be evident later on, we do not need to specify the distribution of their transverse momenta, which is denoted as $P(p_T)$. Thus, the distribution function of

*weronika.jas@gmail.com
†mrow@fuw.edu.pl

partons, which obeys the collisionless Boltzmann equation, is

$$f(t,\mathbf{r},\mathbf{p}) = \frac{1}{\sigma_x\sigma_y\sigma_z\,\Delta Y\langle p_T\rangle}\exp\left[-\frac{(x-v_x t)^2}{2\sigma_x^2}-\frac{(y-v_y t)^2}{2\sigma_y^2}-\frac{(z-v_z t)^2}{2\sigma_z^2}-\frac{Y^2}{2\Delta Y^2}\right]\frac{P(p_T)}{p_T^2\,\mathrm{ch}Y}, \tag{1}$$

where

$$\langle p_T\rangle \equiv \int_0^\infty dp_T\, p_T P(p_T), \qquad \int_0^\infty dp_T\, P(p_T) = 1,$$

and the velocities v_x, v_y, and v_z are given as

$$v_x = \frac{\cos\phi}{\mathrm{ch}Y}, \qquad v_y = \frac{\sin\phi}{\mathrm{ch}Y}, \qquad v_z = \mathrm{th}Y,$$

with ϕ being the azimuthal angle in the momentum space. We note that we use natural units, where $c = 1$. The distribution function is normalized to unity, i.e.,

$$\int d^3r\,\frac{d^3p}{(2\pi)^3}\,f(t,\mathbf{r},\mathbf{p}) = 1.$$

When the impact parameter of the colliding nuclei is chosen to be along the x axis, as shown in Fig. 1, the eccentricity, which drives the elliptic flow, is defined as

$$\varepsilon = \frac{\langle y^2\rangle - \langle x^2\rangle}{\langle y^2\rangle + \langle x^2\rangle}. \tag{2}$$

With the distribution function (1), one computes

$$\langle x^2\rangle \equiv \int d^3r\,\frac{d^3p}{(2\pi)^3}\,x^2 f(t,\mathbf{r},\mathbf{p}) = \sigma_x^2 + \alpha t^2,$$

where

$$\alpha = \frac{1}{2\sqrt{2\pi}\,\Delta Y}\int_{-\infty}^{+\infty}\frac{dY}{\mathrm{ch}^2 Y}\exp\left[-\frac{Y^2}{2\Delta Y^2}\right].$$

If one takes into account only partons with the rapidities Y obeying $Y_{\min} < Y < Y_{\max}$, the formula, which defines the coefficient α, changes to

$$\alpha = \frac{\int_{Y_{\min}}^{Y_{\max}} dY\,\mathrm{ch}^{-2}Y\exp\left[-\frac{Y^2}{2\Delta Y^2}\right]}{2\int_{Y_{\min}}^{Y_{\max}} dY\exp\left[-\frac{Y^2}{2\Delta Y^2}\right]}.$$

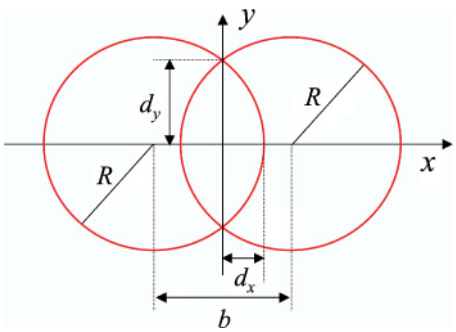

FIG. 1. (Color online) View of colliding nuclei of equal radius R, as seen in the x-y plane transverse to the beam axis.

Computing $\langle y^2\rangle$ analogously to $\langle x^2\rangle$, one finds the eccentricity (2) as

$$\frac{\varepsilon(t)}{\varepsilon(0)} = \left(1+\frac{\alpha}{R_T^2}t^2\right)^{-1}, \tag{3}$$

where the initial eccentricity $\varepsilon(0)$ and the average transverse size of the overlap region of colliding nuclei R_T are

$$\varepsilon(0) = \frac{\sigma_y^2-\sigma_x^2}{\sigma_y^2+\sigma_x^2}, \qquad R_T^2 \equiv \frac{\sigma_y^2+\sigma_x^2}{2}.$$

The formula (3) was earlier derived in Refs. [2,7] for a narrow interval around $Y = 0$ when $\alpha = 1/2$. Unfortunately, by mistake, $\alpha = 1$ in Ref. [7].

When the impact parameter varies, both the initial eccentricity $\varepsilon(0)$ and the average transverse size R_T change. To express the two quantities through the nuclear radius R (a hard sphere parametrization is adopted here) and the impact parameter b, we replace the overlap region of the two circles shown in Fig. 1 by the ellipse given by the equation

$$\frac{x^2}{d_x^2}+\frac{y^2}{d_y^2} \leqslant 1,$$

with the half-axes d_x and d_y defined in Fig. 1. Elementary geometric arguments provide $d_x = R - b/2$ and $d_y = \sqrt{R^2 - b^2/4}$. Since the mean square sizes of the ellipse are $\langle x^2\rangle = d_x^2/4$ and $\langle y^2\rangle = d_y^2/4$, we identify σ_x and σ_y with $d_x/2$ and $d_y/2$, respectively. Then, one expresses $\varepsilon(0)$ and R_T through R and b as

$$\varepsilon(0) = \frac{b}{2R}, \qquad R_T^2 = \frac{R^2}{4}(1-\varepsilon(0)).$$

In Fig. 2, we show predictions of Eq. (3) for Au-Au collisions at midrapidity ($\alpha = 1/2$). The radius of a gold nucleus is chosen to be 7 fm. As seen in Fig. 2, the larger initial eccentricity, the faster its decay. We note that the largest elliptic flow in Au-Au collisions is observed at $b \approx 10$ fm [8]

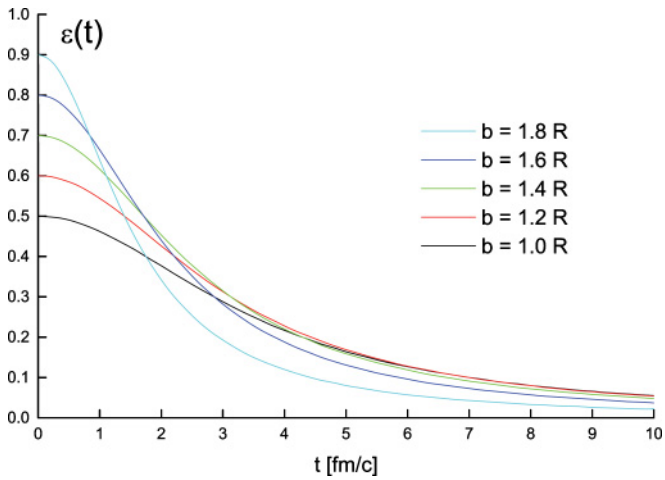

FIG. 2. (Color online) Eccentricity in Au-Au collisions as a function of time for five values of the impact parameter. The curve with the largest initial eccentricity corresponds to $b = 1.8R$, the next one to $b = 1.6R$, etc.

corresponding to $b \approx 1.4R$. At larger impact parameters, the produced system is presumably too small to fully manifest collective hydrodynamic behavior. An analysis of the experimental elliptic flow data within the hydrodynamic model shows that the eccentricity cannot be reduced to less than 75% of its initial value [4], see also Ref. [9]. When the reduction is larger, the ideal hydrodynamics, which gives an upper limit of the flow, significantly underestimates experimental data. Figure 2 shows that for $b \approx 1.4R$, the eccentricity is reduced to 75% of its initial value at 1.5 fm/c. Within this time interval, the system has to be equilibrated to start the hydrodynamic evolution responsible for the elliptic flow. Thus, our estimate of the upper limit of equilibration time is 1.5 fm/c. Actually, the hydrodynamic analysis [4], which uses not only the elliptic flow data but other experimental constraints as well, provides the equilibration time $t_{\rm eq}$ as short as 0.6 fm/c.

III. MOMENTUM ANISOTROPY EVOLUTION

In this section, we compute the momentum distribution of partons in a box of sizes L_x, L_y, and L_z. The box is centered at $x = y = z = 0$. To simplify the calculations, the sharp-edge box is replaced by the box function of Gaussian form

$$\mathcal{O}(\mathbf{r}) = \mathcal{O}_x(x)\mathcal{O}_y(y)\mathcal{O}_z(z), \quad \mathcal{O}_i(r_i) = \sqrt{\frac{6}{\pi}}\exp\left[-\frac{6r_i^2}{L_i^2}\right], \quad i = x, y, z, \tag{4}$$

which obeys the conditions

$$\int_{-L_i/2}^{L_i/2} dr_i = \int dr_i \mathcal{O}_i(r_i), \quad \int_{-L_i/2}^{L_i/2} dr_i r_i^2 = \int dr_i\, r_i^2 \mathcal{O}_i(r_i).$$

The momentum distribution of particles in the box is characterized by the parameter

$$\rho(t) = \frac{2\langle p_z^2\rangle}{\langle p_T^2\rangle}, \tag{5}$$

where

$$\langle p_z^2\rangle = \frac{1}{n}\int d^3r\mathcal{O}(\mathbf{r})\frac{d^3p}{(2\pi)^3}\, p_z^2 f(t, \mathbf{r}, \mathbf{p}),$$
$$n = \int d^3r\mathcal{O}(\mathbf{r})\frac{d^3p}{(2\pi)^3}\, f(t, \mathbf{r}, \mathbf{p}),$$

with analogous formulas for $\langle p_T^2\rangle$; $f(t, \mathbf{r}, \mathbf{p})$ is given by Eq. (1). For the prolate distribution, one has $\rho > 1$; for the isotropic one, $\rho = 1$; and finally, for the oblate distribution, $\rho < 1$. Since the parameter ρ is sensitive only to the second moments of the momentum distribution, $\rho = 1$ is a necessary but not a sufficient condition for an isotropy of the distribution.

The calculations simplify when the system is cylindrically symmetric in coordinate space that is $\sigma_x = \sigma_y = \sigma_T$ and $L_x = L_y = L_T$. Then, the anisotropy parameter (5) is given by

$$\rho(t) = \frac{\int dY\, \mathrm{sh}^2 Y\, G(t, Y)}{\int dY G(t, Y)}, \tag{6}$$

where

$$G(t, Y) \equiv \exp\left[-6\left(\frac{1}{L_T^2 + 12\sigma_T^2}\frac{1}{\mathrm{ch}^2 Y} + \frac{1}{L_z^2 + 12\sigma_z^2}\mathrm{th}^2 Y\right)t^2 - \frac{Y^2}{2\Delta Y^2}\right].$$

One easily computes the initial value of ρ as $\rho(0) = e^{2\Delta Y^2} - 1$. It is also of interest to see how the energy density $e(t)$ in the box decreases when the momentum anisotropy evolves. A simple calculation provides

$$\frac{e(t)}{e(0)} = \frac{e^{-\Delta Y^2/2}}{\sqrt{2\pi}\Delta Y}\int dY \mathrm{ch} Y G(t, Y).$$

To compute $\rho(t)$ and $e(t)/e(0)$, the parameters σ_T, σ_z, L_T, and L_z have to be chosen. As is well known, the nuclear density of heavy nuclei is well described by the Woods-Saxon formula which can be roughly approximated by the sharp-sphere parametrization with the radius R which for the heaviest nuclei equals about 7 fm. The mean square radius for the sharp-sphere parametrization $\langle \mathbf{r}^2\rangle = 3R^2/5$. Therefore, we choose the widths of the Gaussian distribution $\sigma_T = \sigma_x = \sigma_y$ to be equal to $R/\sqrt{5} \approx 3$ fm. The transverse size of the box L_T is assumed to coincide with σ_T. The longitudinal width of the interaction zone σ_z is chosen as 1 fm. The calculations of $\rho(t)$ and $e(t)/e(0)$ are performed for $L_z = 1$ fm and $L_z = 3$ fm. The results are shown in Figs. 3–6.

As already mentioned, the width of rapidity distribution of charged pions produced in Au-Au collisions at $\sqrt{s} = 200$ GeV is $\Delta Y = 2.3$ [6]. One expects that the rapidity of produced partons is even broader. Therefore, the results shown in Figs. 3 and 4 for $\Delta Y = 2.5$ seem to be relevant for heavy-ion collisions at the BNL Relativistic Heavy Ion Collider (RHIC). In such a case, it takes 6–8 fm/c to have an oblate momentum distribution. As Figs. 5 and 6 show, the energy density in the box is then decreased by a large factor—the system is much diluted.

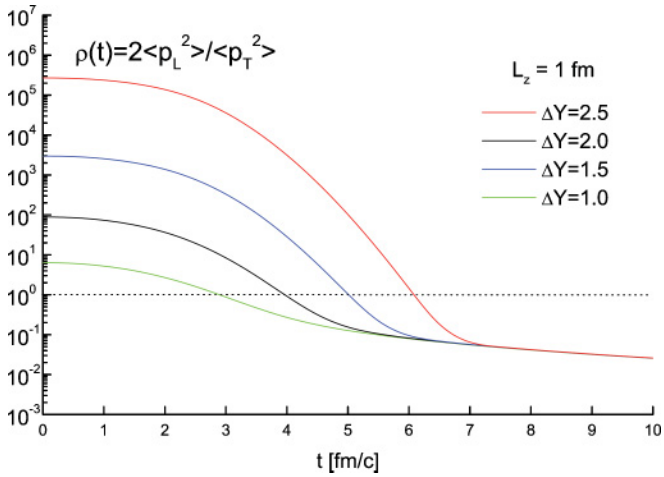

FIG. 3. (Color online) Momentum anisotropy as a function of time for four values of the rapidity distribution width ΔY. The upper most line corresponds to $\Delta Y = 2.5$, the next lower one to $\Delta Y = 2.0$, etc. The longitudinal size of the box L_z equals 1 fm.

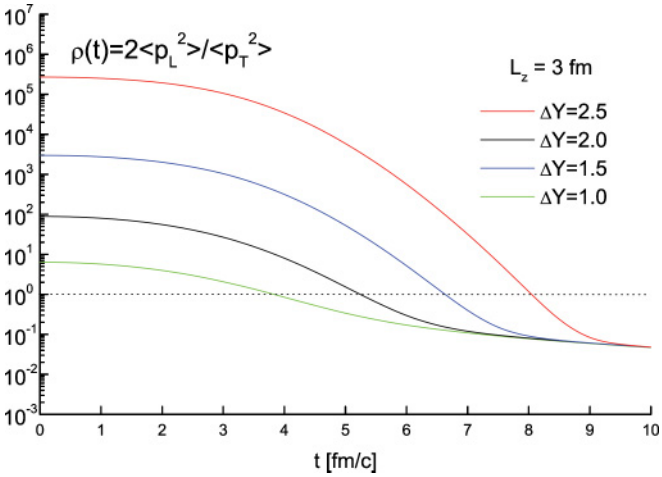

FIG. 4. (Color online) Same as Fig. 3, but for $L_z = 3$ fm.

One argues that particles which are produced with rapidity Y materialize only at a finite proper time τ and space-time rapidity $\eta = Y$. Keeping in mind that

$$\tau = \sqrt{t^2 - z^2}, \quad \eta = \frac{1}{2}\ln\frac{t+z}{t-z},$$

one finds

$$t = \tau\ \mathrm{ch}\eta, \quad z = \tau\ \mathrm{sh}\eta.$$

When the formation time τ is 0.3 fm/c and $\eta = Y = 2.5$, one obtains $t = 1.8$ fm/c and $z = 1.8$ fm. Thus, partons with $Y = 2.5$ materialize beyond the box of $L_z \leqslant 1$ fm. To take into account the effect of finite time formation in our analysis, we simply eliminate from the distribution function (1) the partons of the proper time smaller than τ. In other words, function (1) is multiplied by $\Theta(t\sqrt{1 - v_z^2} - \tau)$, and high-rapidity partons are effectively excluded.

The temporal evolution of the momentum asymmetry ρ, which takes into account the finite formation time, is shown in Figs. 7 and 8 for $\tau = 0.3$ and $\tau = 0.8$ fm/c, respectively. As

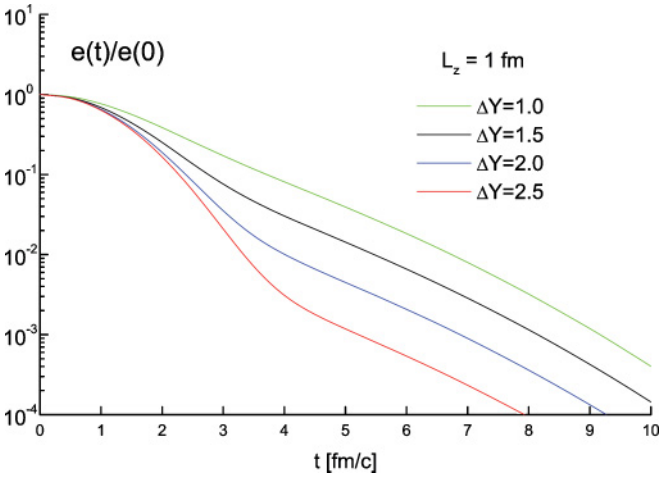

FIG. 5. (Color online) Relative energy density as a function of time for four values of the rapidity distribution width ΔY. The upper most line corresponds to $\Delta Y = 1.0$, the next lower one to $\Delta Y = 1.5$, etc. The longitudinal size of the box L_z equals 1 fm.

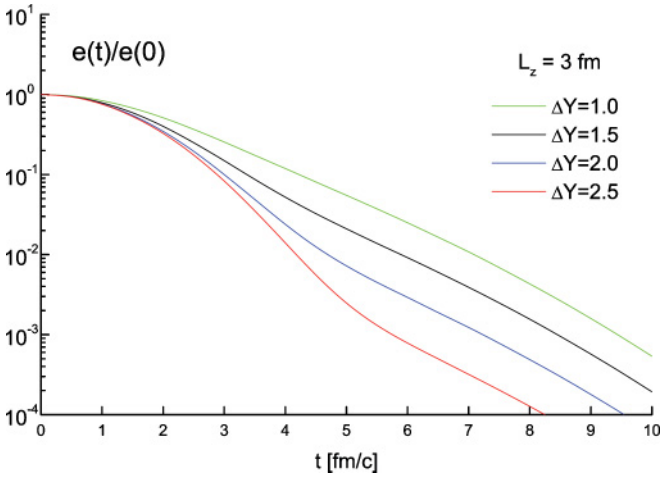

FIG. 6. (Color online) Same as Fig. 5, but for $L_z = 3$ fm.

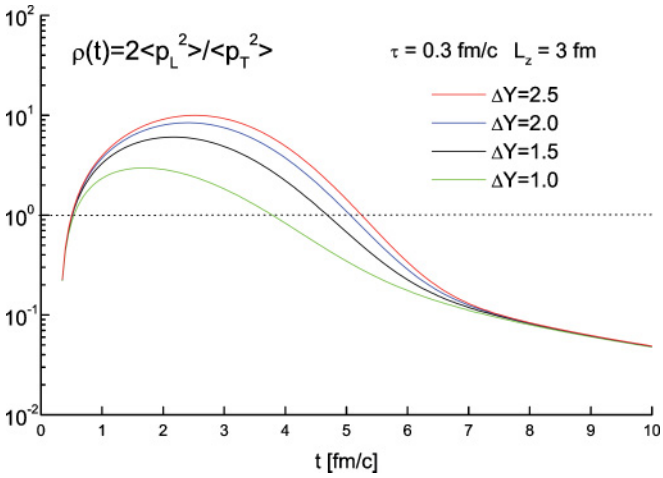

FIG. 7. (Color online) Momentum anisotropy as a function of time for the formation time $\tau = 0.3$ fm/c and four values of the rapidity distribution width ΔY. The upper most line corresponds to $\Delta Y = 2.5$, the next lower one to $\Delta Y = 2.0$, etc. The longitudinal size of the box L_z equals 3 fm.

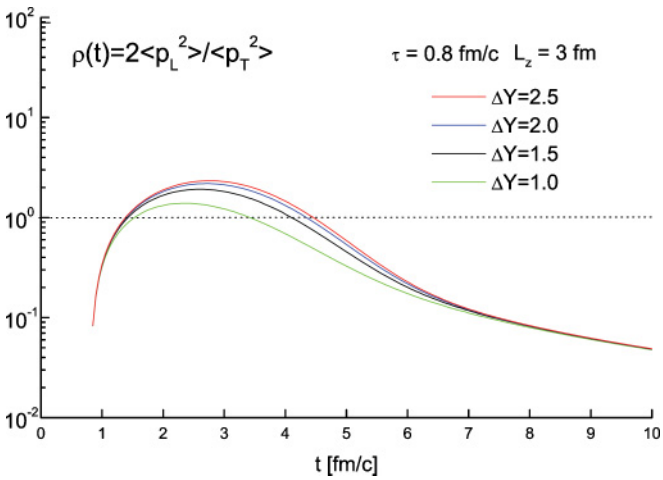

FIG. 8. (Color online) Same as Fig. 7, but for $\tau = 0.8$ fm/c.

previously, $\sigma_T = L_T = 3$ fm, $\sigma_z = 1$ fm, and $L_z = 3$ fm. As seen, the effect of finite formation time is very significant. At the beginning, the momentum distribution is oblate as partons with small Y appear in the box earlier than those with larger Y. After some time, the momentum distribution is prolate, and it becomes again oblate due to the system's expansion only after 3–5 fm/c.

IV. CONCLUSIONS AND DISCUSSION

As discussed in Sec. II, the parton system produced in nucleus-nucleus collisions has to be equilibrated before 1.5 fm/c. Otherwise, the eccentricity is reduced too much, and the ideal hydrodynamics significantly underestimates the experimental data of the elliptic flow. The results from Sec. III show that at the time 1.5 fm/c, the local momentum distribution is still prolate. Therefore, we conclude that just before local equilibrium is reached, the parton momentum distribution is elongated along the beam.

Let us now consider the reliability of this conclusion. First of all, if our rather conservative estimate of the upper limit of equilibration time of $t_{\rm eq} = 1.5$ fm/c is replaced by more elaborated estimate of 0.6 fm/c given in Ref. [4], our conclusion is really safe—it seems impossible to build up the oblate momentum distribution in such a short time.

One wonders whether the formation time τ can be extended. It should be remembered, however, that for finite τ, the initial coordinate space eccentricity does not occur at $t = 0$ but rather at $t = \tau$ (for midrapidity particles). And the interval of time when the system reaches equilibrium is reduced to $t_{\rm eq} - \tau$. So, the longer the τ, the more difficult it is to understand the fast thermalization.

Temporal evolution of the momentum anisotropy is faster when σ_z, which is the initial longitudinal localization of produced partons, is reduced. However, for $L_z = 3$ fm, the time when $\rho = 1$ is shorter only by 25% when σ_z decreases from 1 to 0.5 fm. So, our conclusion remains unchanged. We note that σ_z should not be confused with the longitudinal localization of valence quarks of incoming nuclei which, due to the Lorentz contraction, is σ_T/γ with γ being the Lorentz factor. Our σ_z corresponds to the *produced* partons. Therefore, it cannot be too small, as the wee partons, which are localized beyond the contracted volume of incoming nuclei, effectively participate in nucleus-nucleus collisions.

Our free-streaming model of massless partons is obviously very naive. Partons, which are produced at the collision's early stage, often carry a large virtuality acting as a mass. If the parton mass is taken into account, both the coordinate and momentum space evolutions are slowed down. Interparton interactions presumably lead to a similar effect. However, we cannot see a good reason for why the coordinate space evolution is slowed down much more than the momentum space evolution. Therefore, our conclusion seems to be rather safe.

Obviously, it is desirable to improve our free-streaming model, but the problem is rather difficult. The color glass condensate (CGC) approach (for a review, see Ref. [10]), which is the best developed effective theory for studying the early stage of heavy-ion collision, is not well suited for the problem. The valence quarks are treated in CGC as classical passive sources of small x, highly populated gluons which are described in terms of classical fields. Partons with sizable x, which crucially influence the momentum distribution, are essentially absent in CGC.

Numerous studies of equilibration of parton systems with the initially oblate momentum distribution, which are reviewed in Ref. [1], are theoretically well founded as the oblate system is diluted and decohered. However, according to our conclusion, these studies do not actually explain how local equilibrium is reached in heavy-ion collisions but rather how the equilibrium is sustained. We believe that the plasma equilibration, in particular the color instabilities, which are supposed to speed up the process of thermalization, should be analyzed as in Refs. [11,12], that is, in the systems with prolate momentum distribution. We are aware that kinetic theory is hardly applicable to such dense, inhomogeneous, and partially coherent systems, but Nature does not seem to be bothered by our theoretical difficulties.

ACKNOWLEDGMENTS

We are grateful to Ulrich Heinz for helpful correspondence. This work was partially supported by the Polish Ministry of Science and Higher Education under Grant 1 P03B 12730.

[1] St. Mrówczyski, Acta Phys. Pol. B **37**, 427 (2006).
[2] P. F. Kolb and U. W. Heinz, in *Quark Gluon Plasma 3*, edited by R. C. Hwa and X. N. Wang (World Scientific, Singapore, 2004).
[3] P. Arnold, J. Lenaghan, G. D. Moore, and L. G. Yaffe, Phys. Rev. Lett. **94**, 072302 (2005).
[4] U. W. Heinz, AIP Conf. Proc. **739**, 163 (2005).
[5] St. Mrówczyński and P. Danielewicz, Nucl. Phys. **B342**, 345 (1990).
[6] I. G. Bearden *et al.* (BRAHMS Collaboration), Phys. Rev. Lett. **94**, 162301 (2005).
[7] P. F. Kolb, J. Sollfrank, and U. W. Heinz, Phys. Rev. C **62**, 054909 (2000).
[8] C. Adler *et al.* (STAR Collaboration), Phys. Rev. C **66**, 034904 (2002).
[9] H. J. Drescher, A. Dumitru, C. Gombeaud, and J. Y. Ollitrault, Phys. Rev. C **76**, 024905 (2007).
[10] E. Iancu and R. Venugopalan, in *Quark Gluon Plasma 3*, edited by R. C. Hwa and X. N. Wang (World Scientific, Singapore, 2004).
[11] St. Mrówczyński, Phys. Rev. C **49**, 2191 (1994).
[12] J. Randrup and St. Mrówczyński, Phys. Rev. C **68**, 034909 (2003).